Rarefied planar jet and jet impingement flows

C. Cai, C. Zou, X. Huang, L. Wang, and Q. Sun

Citation: AIP Conference Proceedings **1501**, 1249 (2012); doi: 10.1063/1.4769685
View online: http://dx.doi.org/10.1063/1.4769685
View Table of Contents: http://scitation.aip.org/content/aip/proceeding/aipcp/1501?ver=pdfcov
Published by the AIP Publishing

This article is copyrighted as indicated in the article. Reuse of AIP content is subject to the terms at: http://scitation.aip.org/termsconditions. Downloaded to IP: 159.226.100.225 On: Tue, 14 Jan 2014 01:44:34

Rarefied Planar Jet and Jet Impingement Flows

C. Cai[a], C. Zou[a], X. Huang[a], L. Wang[a], Q. Sun[b]

[a]*Department of Mechanical and Aerospace Engineering, New Mexico State University, Las Cruces, New Mexico 88003*
[b]*Laboratory of High Temperature Gas Dynamics, Institute of Mechanics, Chinese Academy of Sciences, Beijing, P.R. China*

Abstract. This paper presents three sets of analytical exact solutions to collisionless gas flows from a two-dimensional exit. The first set is free plume expanding into a vacuum, and the other two sets are collisionless plume impingement at a vertically set plate. Both diffuse and specular plate surface reflections are considered for the plume impingement problem. Numerical simulations with the direct simulation Monte Carlo method are used to provide several test cases, the flow field properties are obtained, and very good agreement is observed between the exact and numerical simulations.

Keywords: Gaskinetic Theory, Rarefied, Jet, Plume Impingement, Monte Carlo Methods, Vacuum, DSMC, Simulation
PACS: 82.40-g, 51.10.+y, 98.58.fd, 98.38.Fs, 52.65.Pp, 52.55.Fa, 07.30.Dz, 52.25.Ya, 47.60.Kz, 47.45.-n, 52.25.Ya.

INTRODUCTION

The problems of gaseous jet and jet impingement at a normally set plate are two fundamental fluid dynamic problems, and there are many applications in aerospace/mechanical/chemical engineering, physics and chemistry.

As the counterpart to the continuum flow limit, the exact solutions to the highly rarefied jet and jet impingement flows provide another bounding limit to these flows. Even though they are complex, they provide some insights to many problems by only including molecular movement. In many applications, the contribution from inter-particle collisions is insignificant. For example, they are related to the atomic/molecular beams [1,2] which is a crucial tool responsible for many important discoveries. Another important application includes materials processing inside vacuum chambers [3], and rocket plume effects [4]. Due to the importance and numerous applications, rarefied gaseous plume flows have been investigated for decades.

For jet and jet impingement at a plate, there are many studies based on continuum theory, for example, the Navier-Stokes equations, boundary layer theory, characteristic lines, Prandtl-Meyer expansions. For collisionless regime, there are many numerical and experimental studies and reports for the complete flow field and surface properties. For high speed gaseous collisionless flows out of an exit, most of the past studies adopted some simplifications. For example, Noller [5] proposed a solid angle treatment to implicitly consider the nozzle exit geometry. The cosine law or the Simons plume model [6] treats a rocket plume as from a point source; Narasimha's early investigation [7] indicated that the plume solution is rather complicated with many cosine functions. Another rocket plume treatment, which is one-dimensional, unsteady, and based on collisionless flows, was adopted by Woronowicz [8]. His treatment splits the exit into many small segments, as such, the density and pressure distributions in the flowfield can be computed numerically. Furthermore, he adopted the concept of starter surface, which alleviates the difficulty of this problem. Dettleef provided a comprehensive review on rocket plume and plume impingement flows [9].

This paper summarizes some recent work on highly rarefied gaseous planar jet and jet impingement flow solutions. Section II presents the exact solutions to collisionless planar jet expanding into a vacuum; Section III presents the exact solutions to collisionless two dimensional jet impingement at a normally set flat plate with diffuse reflections; Section IV reports some development on impingement at a specular reflection plate; Section V includes comparison of the exact analytical solutions and the DSMC [10] simulation results of collisionless plume and plume impingement flows; the last section VI summarizes this paper with a few conclusions.

COLLISIONLESS FREE PLUME EXPANDING INTO A VACUUM

The first problem is a collisionless free plume expanding into a vacuum from a planar nozzle with a mean macroscopic velocity of U_0 . The results are the foundations to study the problems in the next two sections.

28th International Symposium on Rarefied Gas Dynamics 2012
AIP Conf. Proc. 1501, 1249-1256 (2012); doi: 10.1063/1.4769685
© 2012 American Institute of Physics 978-0-7354-1115-9/$30.00

This article is copyrighted as indicated in the article. Reuse of AIP content is subject to the terms at: http://scitation.aip.org/termsconditions. Downloaded to IP: 159.226.100.225 On: Tue, 14 Jan 2014 01:44:34

Figure 1 illustrates the problem and the thermal velocity domain for a point, *P*(*X, Y*), in the flowfield. Ω_1 in Fig. 1(b) is a specific region related to the solid angle which is subtended by the flowfield point *P*(*X,Y*) and the nozzle exit lips in Fig. 1(a). Those molecules leaving the nozzle exit are characterized by the following zero-velocity centered Maxwellian distribution function:

$$f_0(0,y,z) = n_0(\beta_0/\pi)^{3/2}\exp[-\beta_0(u^2+v^2+w^2)], \tag{1}$$

where n_0 is the exit number density, and $\beta_0 = 1/(2RT_0)$.

The velocity components of those particles arriving at point *P*(*X, Y*) must satisfy the following constrain relation:

$$\tan\theta = \frac{Y-y}{X} = \frac{v}{u+U_0}. \tag{2}$$

Based on the gaskinetic relations, the final results for the flowfield density, velocity, and temperatures are derived as [11]:

$$\frac{n_1(X,Y)}{n_0} = \frac{\exp(-S_0^2)}{2\pi}(\theta_2-\theta_1) + \frac{1}{4}\left[\mathrm{erf}(S_0\sin\theta_2) - \mathrm{erf}(S_0\sin\theta_1)\right] + \frac{S_0}{2\sqrt{\pi}}\int_{\theta_1}^{\theta_2}\exp(-S_0^2\sin^2\theta)\cos\theta\,\mathrm{erf}(S_0\cos\theta)\,d\theta, \tag{3}$$

$$U_1(X,Y)\sqrt{\beta_0} = \frac{\exp(-S_0^2)}{2\pi}\frac{n_0}{n_1}\left\{\begin{array}{l}\frac{1}{2}S_0(\theta_2-\theta_1)+\frac{1}{4}S_0\left[\sin(2\theta_2)-\sin(2\theta_1)\right]\\ +\frac{\sqrt{\pi}}{2}\int_{\theta_1}^{\theta_2}(1+2S_0^2\cos^2\theta)\cos\theta\exp(S_0^2\cos^2\theta)\left[1+\mathrm{erf}(S_0\cos\theta)\right]d\theta\end{array}\right\}, \tag{4}$$

$$V_1(X,Y)\sqrt{\beta_0} = \frac{1}{4\sqrt{\pi}}\frac{n_0}{n_1}\left\{\exp(-S_0^2\sin^2\theta_1)\cos\theta_1\left[1+\mathrm{erf}(S_0\cos\theta_1)\right] - \exp(-S_0^2\sin^2\theta_2)\cos\theta_2\left[1+\mathrm{erf}(S_0\cos\theta_2)\right]\right\}, \tag{5}$$

$$T_1(X,Y)/T_0 = -\frac{U_1^2+V_1^2}{3RT_0} + \frac{\exp(-S_0^2)}{6\pi}\frac{n_0}{n_1}\left\{\begin{array}{l}(3+S_0^2)(\theta_2-\theta_1)+\frac{1}{2}S_0^2\left[\sin(2\theta_2)-\sin(2\theta_1)\right]+\\ 2\sqrt{\pi}\int_{\theta_1}^{\theta_2}(2+S_0^2\cos^2\theta)S_0\cos\theta\exp(S_0^2\cos^2\theta)\left[1+\mathrm{erf}(S_0\cos\theta)\right]d\theta\end{array}\right\}, \tag{6}$$

with the following definitions:

$$\tan\theta_1 = \frac{Y-H}{X}, \quad \tan\theta_2 = \frac{Y+H}{X}. \tag{7}$$

These formulas illustrate that the free plume flowfield solutions contain geometry factors of *X, Y,* and the velocity speed ratio $S_0=U_0/(2RT_0)^{1/2}$, and here we define $A(x) = 1+\mathrm{erf}(S_0\cos(x))$.

COLLISIONLESS PLANAR JET IMPINGEMENT AT A NORMALLY SET DIFFUSE PLAT

Figure 2 shows the problem of jet impingement at a diffuse plate and the corresponding velocity phase. A high speed gaseous jet fires from a nozzle with a width of 2H, the molecules at the nozzle exit are characterized by a number density n_0, a mean velocity U_0, and a temperature T_0. The contribution to the flow field properties are essentially from two different sources, the free plume from the planar nozzle exit, and the plate surface. They are represented by Ω_1 and Ω_2 respectively in Fig. 2(b).

We assume the velocity distribution function for those reflected particles from the diffuse surface is:

$$f_w(Y) = n_w(Y)\frac{\beta_w}{\pi}\exp\left[-\beta_w(c_1^2+c_2^2)\right], \tag{8}$$

where $n_w(Y)$ has a distribution along the surface and it is the only property to be determined by using the condition of zero flux at the plate surface. Integration with *u* as the moment yields the following relation about n_w:

$$n_1(L,Y)U_1(L,Y) = \frac{n_w\sqrt{RT_w}}{\sqrt{2\pi}}. \tag{9}$$

The slip velocity at the plate is:

$$V_2(L,Y) = \frac{\sqrt{RT_w}V_1(L,Y)}{\sqrt{RT_w}+\sqrt{\pi/2}U_1(L,Y)}. \tag{10}$$

This article is copyrighted as indicated in the article. Reuse of AIP content is subject to the terms at: http://scitation.aip.org/termsconditions. Downloaded to IP: 159.226.100.225 On: Tue, 14 Jan 2014 01:44:34

Following the same approach in solving the problem of a free plume expanding into a vacuum, we obtain the number density, velocity components, and temperature distributions of the flow field for the second problem [12]:

$$n_2(X,Y) = n_1(X,Y) + \frac{L-X}{2\pi}\int_{-W}^{W} \frac{n_w(y_0)}{(Y-y_0)^2+(X-L)^2}\,dy_0, \tag{11}$$

$$U_2(X,Y) = \left[n_1(X,Y)U_1(X,Y) + \frac{(L-X)^2}{4\sqrt{\pi\beta_w}}\int_{-W}^{W} \frac{n_w(y_0)}{\left[(Y-y_0)^2+(X-L)^2\right]^{\frac{3}{2}}}\,dy_0 \right] \Big/ n_2(X,Y), \tag{12}$$

$$V_2(X,Y) = \left[n_1(X,Y)V_1(X,Y) + \frac{L-X}{4\sqrt{\pi\beta_w}}\int_{-W}^{W} \frac{n_w(y_0)(Y-y_0)}{\left[(Y-y_0)^2+(X-L)^2\right]^{\frac{3}{2}}}\,dy_0 \right] \Big/ n_2(X,Y), \tag{13}$$

$$T_2(X,Y) = \left[n_1(X,Y)T_1(X,Y) + \frac{1}{2\pi\beta_w}\int_{-W}^{W} \frac{n_w(y_0)}{(Y-y_0)^2+(X-L)^2}\,dy_0 \right] \Big/ n_2(X,Y). \tag{14}$$

The surface pressure, shear stress and heat flux is,

$$C_p = \frac{n_w T_w}{2n_0 T_0} + \frac{\exp(-S_0^2)}{2\pi}\int_{\theta_1}^{\theta_2} \cos^2\theta\{2(1+S_0^2\cos^2\theta) + \sqrt{\pi}S_0\cos\theta(3+2S_0^2\cos^2\theta)\exp(S_0^2\cos^2\theta)A(\theta)\}d\theta, \tag{15}$$

$$C_f = \frac{1}{4\pi S_0^2}\begin{pmatrix} (\cos^2\theta_1 - \cos^2\theta_2)\exp(-S_0^2) + \sqrt{\pi}S_0\cos^3\theta_1\exp(-S_0^2\sin^2\theta_1)A(\theta_1) \\ -\sqrt{\pi}S_0\cos^3\theta_2\exp(-S_0^2\sin^2\theta_2)A(\theta_2) \end{pmatrix}, \tag{16}$$

$$C_q = \frac{\exp(-S_0^2)}{4\pi S_0^2}\begin{pmatrix} \int_{\theta_1}^{\theta_2}\{\frac{\sqrt{\pi}}{S_0}[\frac{3}{2}+6S_0^2\cos^2\theta+2S_0^4\cos^4\theta+(\frac{1}{2}+\beta_0 V_2^2)(1+2S_0^2\cos^2\theta)]\exp(S_0^2\cos^2\theta)A(\theta)+ \\ \cos\theta(6+2S_0^2\cos^2\theta+2\beta_0 V_2^2)\}\cos\theta d\theta - \frac{V_2}{U_0}\int_{\theta_1}^{\theta_2}\sin(2\theta)\{2+2S_0^2\cos^2\theta+ \\ \sqrt{\pi}\exp(S_0^2\cos^2\theta)A(\theta)(3S_0\cos\theta+2S_0^3\cos^3\theta)\}d\theta \end{pmatrix}. \tag{17}$$

COLLISIONLESS PLANAR JET IMPINGEMENT AT A NORMALLY SET SPECULAR PLATE

The problem and the thermal velocity phase pictures for a flowfield point *P*(*X, Y*) between a nozzle and a specular reflective plate, which has a distance of *L* from the nozzle, are illustrated by Fig. 3. In Fig. 3(a), an extra "virtual" nozzle is mirrored at the other side of the plate to satisfy the non-penetration wall condition. The treatment is similar to the point source problem in the potential flow theory.

The normalized density, velocity components, and temperature at point *P*(*X, Y*) are computed as follows:

$$\frac{n_3(X,Y)}{n_0} = \begin{Bmatrix} \frac{\exp(-S_0^2)}{2\pi}(\theta_2-\theta_1+\theta_4-\theta_3) + \frac{1}{4}\left[\operatorname{erf}(S_0\sin\theta_2) - \operatorname{erf}(S_0\sin\theta_1) + \operatorname{erf}(S_0\sin\theta_4) - \operatorname{erf}(S_0\sin\theta_3)\right] \\ + \frac{S_0}{2\sqrt{\pi}}\left[\int_{\theta_1}^{\theta_2}\exp(-S_0^2\sin^2\theta)\cos\theta\operatorname{erf}(S_0\cos\theta)\,d\theta + \int_{\theta 3}^{\theta_4}\exp(-S_0^2\sin^2\theta)\cos\theta\operatorname{erf}(S_0\cos\theta)\,d\theta\right] \end{Bmatrix}, \tag{18}$$

$$U_3(X,Y)\sqrt{\beta_0} = \frac{\exp(-S_0^2)}{2\pi}\frac{n_0}{n_3}\begin{Bmatrix} \frac{1}{2}S_0(\theta_2-\theta_1+\theta_4-\theta_3) + \frac{1}{4}S_0\left[\sin(2\theta_2)-\sin(2\theta_1)+\sin(2\theta_3)-\sin(2\theta_4)\right] + \\ \frac{\sqrt{\pi}}{2}\int_{\theta_1}^{\theta_2}(1+2S_0^2\cos^2\theta)\cos\theta\exp(S_0^2\cos^2\theta)\left[1+\operatorname{erf}(S_0\cos\theta)\right]d\theta + \\ \frac{\sqrt{\pi}}{2}\int_{\theta 3}^{\theta_4}(1+2S_0^2\cos^2\theta)\cos\theta\exp(S_0^2\cos^2\theta)\left[1-\operatorname{erf}(S_0\cos\theta)\right]d\theta \end{Bmatrix}, \tag{19}$$

This article is copyrighted as indicated in the article. Reuse of AIP content is subject to the terms at: http://scitation.aip.org/termsconditions. Downloaded to IP: 159.226.100.225 On: Tue, 14 Jan 2014 01:44:34

$$V_3(X,Y)\sqrt{\beta_0}=\frac{1}{4\sqrt{\pi}}\frac{n_0}{n_3}\left\{\begin{array}{l}\exp\left(-S_0^2\sin^2\theta_1\right)\cos\theta_1\left[1+\mathrm{erf}\left(S_0\cos\theta_1\right)\right]-\exp\left(-S_0^2\sin^2\theta_2\right)\cos\theta_2\left[1+\mathrm{erf}\left(S_0\cos\theta_2\right)\right]+\\ \exp\left(-S_0^2\sin^2\theta_4\right)\cos\theta_4\left[1-\mathrm{erf}\left(S_0\cos\theta_4\right)\right]-\exp\left(-S_0^2\sin^2\theta_3\right)\cos\theta_3\left[1-\mathrm{erf}\left(S_0\cos\theta_3\right)\right]\end{array}\right\}, \quad (20)$$

$$\frac{T_3(X,Y)}{T_0}=-\frac{U_3^2+V_3^2}{3RT_0}+\frac{\exp\left(-S_0^2\right)}{6\pi}\frac{n_0}{n_3}\left\{\begin{array}{l}\left(3+S_0^2\right)\left(\theta_2-\theta_1+\theta_4-\theta_3\right)+\frac{1}{2}S_0^2\left[\sin\left(2\theta_2\right)-\sin\left(2\theta_1\right)+\sin\left(2\theta_4\right)-\sin\left(2\theta_3\right)\right]\\ +2\sqrt{\pi}\int_{\theta_1}^{\theta_2}\left(2+S_0^2\cos^2\theta\right)S_0\cos\theta\exp\left(S_0^2\cos^2\theta\right)\left[1+\mathrm{erf}\left(S_0\cos\theta\right)\right]d\theta\\ -2\sqrt{\pi}\int_{\theta3}^{\theta_4}\left(2+S_0^2\cos^2\theta\right)S_0\cos\theta\exp\left(S_0^2\cos^2\theta\right)\left[1-\mathrm{erf}\left(S_0\cos\theta\right)\right]d\theta\end{array}\right\}. \quad (21)$$

The plate surface pressure coefficient is:

$$C_p=\frac{\exp(-S_0^2)}{2\pi}\left(\begin{array}{l}\int_{\theta_1}^{\theta_2}\cos^2\theta\{2(1+S_0^2\cos^2\theta)+\sqrt{\pi}S_0\cos\theta(3+2S_0^2\cos^2\theta)\exp(S_0^2\cos^2\theta)A(\theta)\}d\theta+\\ \int_{\theta_3}^{\theta_4}\cos^2\theta\{2(1+S_0^2\cos^2\theta)-\sqrt{\pi}S_0\cos\theta(3+2S_0^2\cos^2\theta)\exp(S_0^2\cos^2\theta)[1-\mathrm{erf}(S_0\cos\theta)]\}d\theta\end{array}\right). \quad (22)$$

VALIDATIONS

This section includes numerical validations using the DSMC method. All simulations are performed with a special DSMC package, GRASP, with the -P module [13].This module is a general purpose particle simulation package with special object-oriented programming styles and software engineering design patterns. In the DSMC simulations for the free plume problem, an inlet boundary represents the nozzle exit at the lower left corner, a symmetric line for the plume centerline and vacuum boundaries for other sides. For the plume impingement problems, a vertical line segment is adopted to represent the diffuse or specular planar plate, which locates at the right side of the simulation domain. For the DSMC simulations in this paper, Knudsen number is set to Kn=100, as such the analytical results are truly collisionless.

Figure 4 compares analytical collisionless flow density results, Eqns.(11) and (18), and the corresponding DSMC simulation results. Due to the plate blockage, particles accumulated in front of the plate and density increases. In general, the agreement is good. Other validation results can be found in other papers [14, 15]. Figure 5 compares analytical collisionless flow u-velocity component contours, Eqs. (12) and (19), and the corresponding DSMC simulation results. Due to the plate blockage, particles' U-velocity decreases from the exit to zero at the plate surface. Figure 6 compares analytical collisionless flow v-velocity component contours, Eqns.(13) and (20), and the DSMC simulation results. Even though the diffuse plate and specular plate results are very similar, there are some noticeable difference between the results of diffuse plate and specular plate. For example, the flow patterns in the specular plate are always symmetric about the plate.

Figure 7 compares analytical results of surface pressures for collisionless flow impingement at a flat plate, Eqns.(15) and (22), and the corresponding results from DSMC simulations. Figure 8 compares analytical results of surface shear stress and heat flux for collisionless flow impingement at a flat diffuse plate, Eqns.(16) and (17), and the corresponding results from DSMC simulations. In general, the agreement is almost identical. Figures 7 and 8 provide one limit for the problem of gaseous jet impingement at a flat plate.

This article is copyrighted as indicated in the article. Reuse of AIP content is subject to the terms at: http://scitation.aip.org/termsconditions. Downloaded to IP: 159.226.100.225 On: Tue, 14 Jan 2014 01:44:34

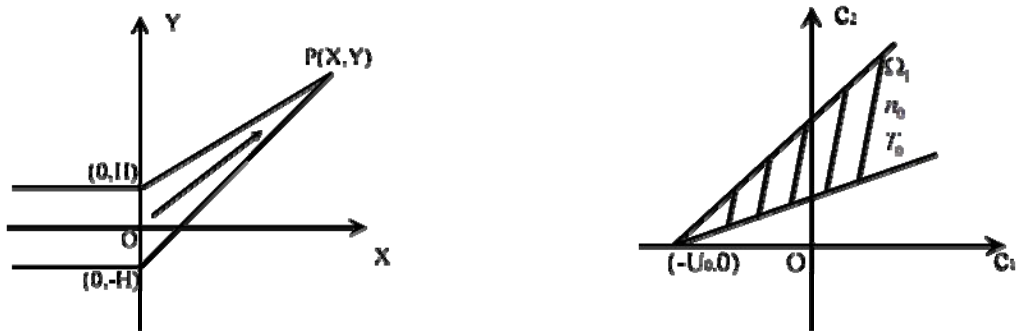

(a) (b)

FIGURE 1. (a) Illustration and (b) thermal velocity phase for the free plume expansion problem.

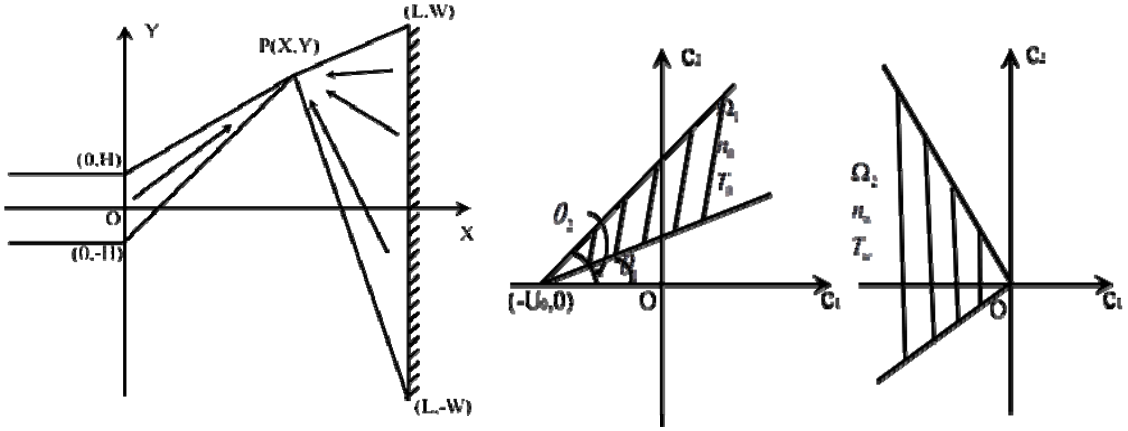

(a) (b)

FIGURE 2. (a) Illustration for the problem of impingement at a diffuse plate and (b) its thermal velocity phase.

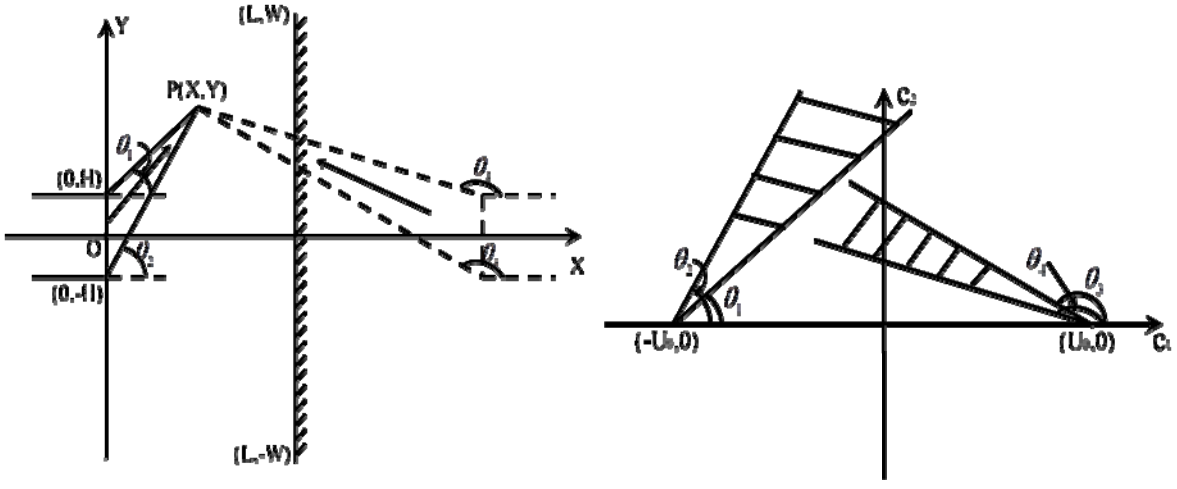

(a) (b)

FIGURE 3. (a) Illustration for the problem of impingement at a specular plate and (b) its thermal velocity phase.

This article is copyrighted as indicated in the article. Reuse of AIP content is subject to the terms at: http://scitation.aip.org/termsconditions. Downloaded to IP: 159.226.100.225 On: Tue, 14 Jan 2014 01:44:34

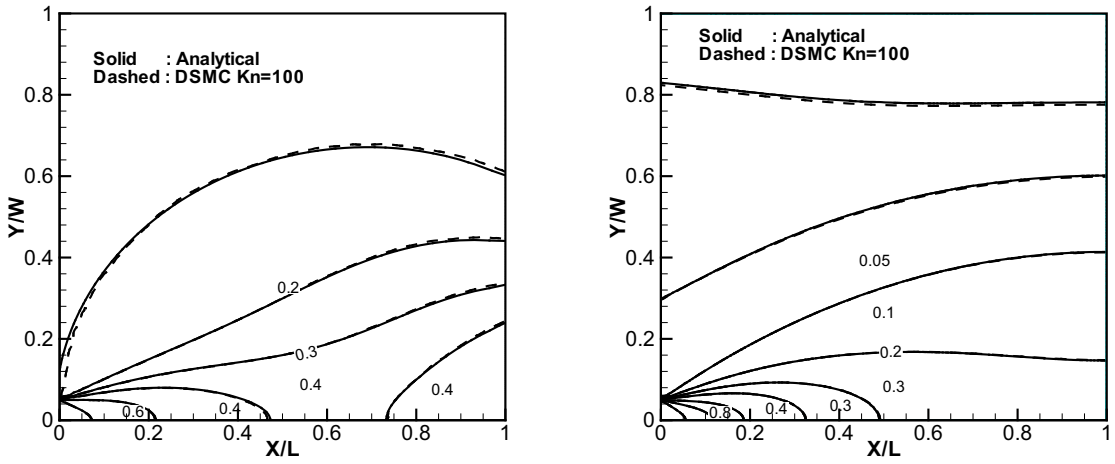

(a) (b)

FIGURE 4. Contours of number density for the impingement problems, (a) diffuse plate; (b) specular plate. S_0=2.

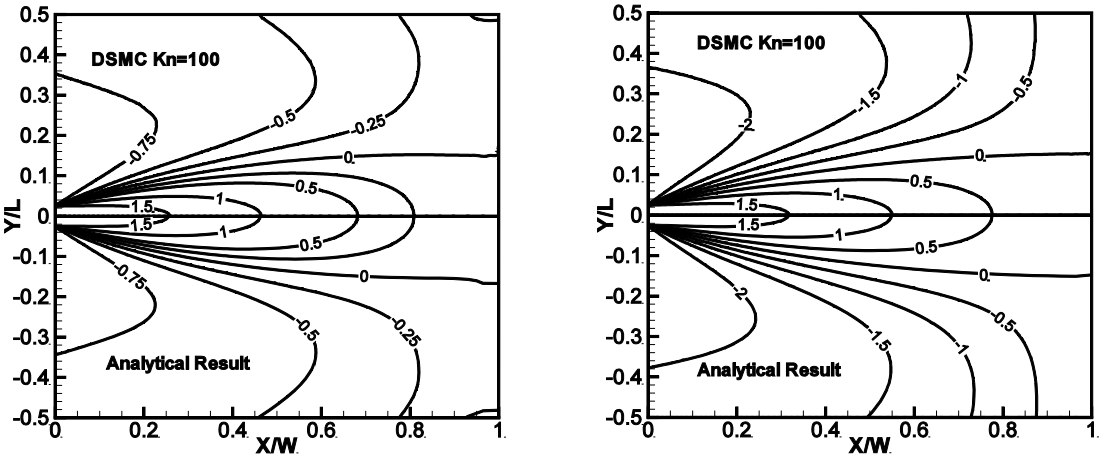

(a) (b)

FIGURE 5. U-velocity component contours for the impingement flow problems, (a) diffuse plate; (b) specular plate. S_0=2.

This article is copyrighted as indicated in the article. Reuse of AIP content is subject to the terms at: http://scitation.aip.org/termsconditions. Downloaded to IP: 159.226.100.225 On: Tue, 14 Jan 2014 01:44:34

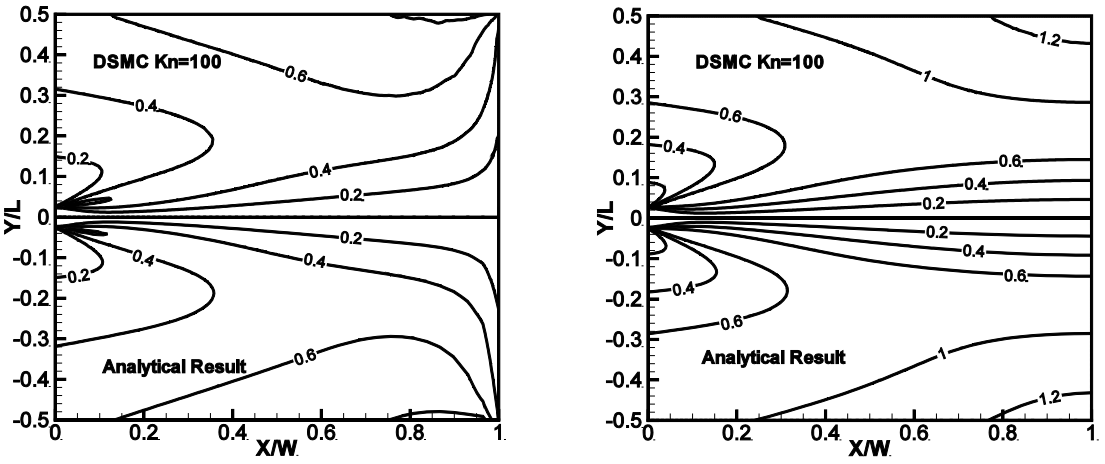

(a) (b)

FIGURE 6. V-velocity component contours for the impingement flow problems, (a) diffuse plate; (b) specular plate. S_0=2.

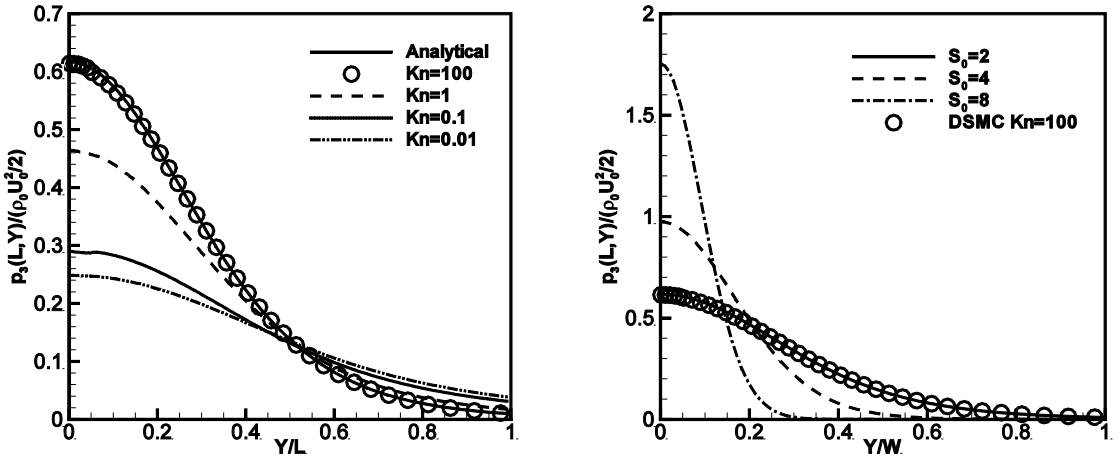

(a) (b)

FIGURE 7. Surface pressure coefficient distributions for the impingement flow problems: (a) diffuse plate; (b) specular plate.

This article is copyrighted as indicated in the article. Reuse of AIP content is subject to the terms at: http://scitation.aip.org/termsconditions. Downloaded to IP: 159.226.100.225 On: Tue, 14 Jan 2014 01:44:34

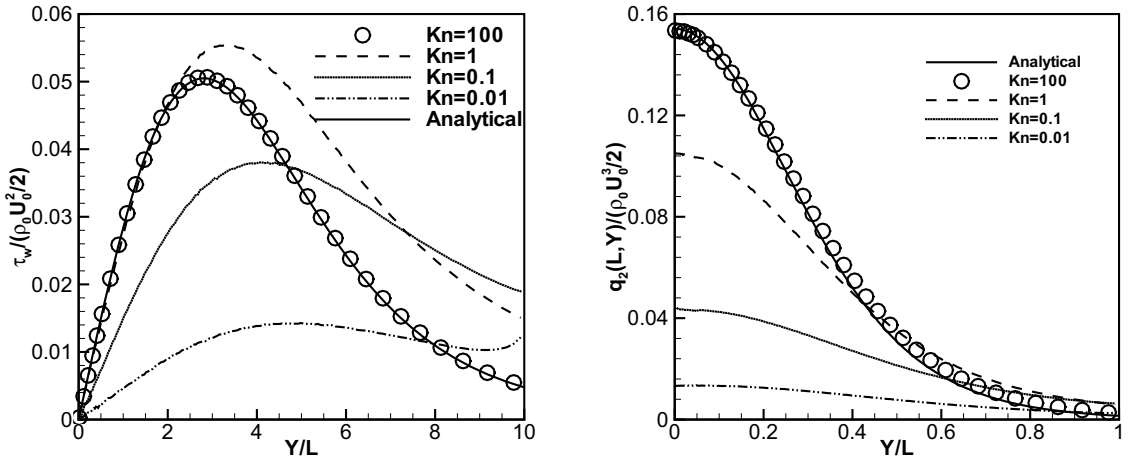

(a) (b)

FIGURE 8. Surface shear stress and heat flux distributions for impingement at a diffuse plate: (a) shear stress; (b) heat flux. S_0=2.

CONCLUSIONS

In this paper, three fundamental problems of collisionless flows are investigated: free jet expanding into a vacuum, free jet impingement at a normally set diffuse reflective flat plate, and free jet impingement at a normally set specular reflective flat plate. A fundamental velocity-space relation is adopted to solve these important flows. Flowfield properties which include number density, velocity, temperature, and pressure formulas are presented for these three fundamental problems. These solutions are the counterpart solutions to the continuum gaseous jet and jet impingement problems, and they provide us some new insights on these fundamental problems.

ACKNOWLEDGMENTS

The authors acknowledge partial funding support from grants NASA-ZTNMSU012209-DUST, NSF-CBET-0854411, and NSF-DMS-0914706.

REFERENCES

1. R. Campargue, Historical Account and Branching to Rarefied Gas Dynamics of Atomic &Molecular Beams: A Continuing and Fascinating Odyssey Commemorated by Nobel Prizes Awarded to 23 Laureates in Physics & Chemistry, AIP Conference Proceedings, Vol. 762, Rarefied Gas Dynamics: *24th International Symposium on Rarefied Gas Dynamics*, Editor: Mario Capitelli, Bari (Italy), 32-44.
2. G. Sanna, and G. Tomassetti, *Introduction to Molecular Beams Gas Dynamics*, London: Imperial College Press, 2005.
3. R. Maev, and V. Leshchynsky, *Introduction to Low Pressure Gas Dynamic Spray*, Weinheim: Wiley-Vch, 2008.
4. G. P. Sutton, and O. Biblarz, *Rocket Propulsion Elements*, 8th edition, New Jersey: John Wiley & Sons, 2010.
5. H. G., Noller, *J. Vac. Sci. Tech*. **3**, 202-207 (1996).
6. G. A., Simons, *AIAA J.* **10**, 1534-1535 (1972).
7. R. Narasimha, *J. Fluid Mech.* **12**, 294-308 (1962).
8. M. S., Woronowicz, AIAA paper 1994-2048 (1994).
9. G. Dettleef, *Prog. Aerospace Sci.* **28**, 1-71 (1991).
10. G. A. Bird, *Molecular Gas Dynamics and the Direct Simulation of Gas Flows*, New York: Oxford University Press, 1994.
11. C. Cai, and I. D. Boyd, *J. Spacecraft Rockets* **44**, 619-624 (2007).
12. K. Khasawneh, H. Liu, and C. Cai*, Phys. Fluids* **23,** 1-6 (2011).
13. H. Liu, C. Cai, and C. Zou, *Comput. Fluids* **57**, 65-75 (2012).
14. C. Cai, and I. D. Boyd, *J. Spacecraft Rockets* **44**, 1326-1330 (2007).
15. C. Cai, and L. Wang, *J. Spacecraft Rockets* **41**, 59-68 (2011).

This article is copyrighted as indicated in the article. Reuse of AIP content is subject to the terms at: http://scitation.aip.org/termsconditions. Downloaded to IP: 159.226.100.225 On: Tue, 14 Jan 2014 01:44:34